




Effects of mass loading on the viability of assessing the state of healing of a fixated fractured long bone

WK Chiu¹ , WH Ong¹ , M Russ^{2,3,4}, T Tran¹ and M Fitzgerald^{2,3,5} 

Abstract

Introduction: This paper aims to evaluate the effects of mass loading on the healing assessment of an internally fixated femur by vibrational means. The presence of soft tissue surrounding a femur increases damping and mass of a system, and hence affects the vibrational response of a mechanical structure by obscuring the coherent modes. This may compromise vibration-based monitoring strategies in identifying modes associated with fracture healing.

Methods: This paper presents a series of experimental works to address this issue. Two osteotomised composite femurs were internally fixated using a plate-screw system and an intramedullary nail. Soft tissue is approximated by surrounding an artificial Sawbone femur with modelling clay. The femur is excited by an instrumented impact hammer and instrumented with two accelerometers to record bending and torsion modes between 0 and 600 Hz. A 30-min epoxy was applied to simulate the healing of the fractured femur in the osteotomised region. The resonant frequencies and its modes are monitored while union is being formed and a healing index is calculated at various times to quantify the degree of healing.

Results: The results demonstrate that the effect of modelling clay compressed the natural modes along the frequency axis. It is observed that frequency bandwidth in the vicinity of 150 Hz and 500 Hz is sensitive to the state of healing of the fixated femurs, which is due to the increase in stiffness of the osteotomised region. These findings were used to formulate the healing index which assists in identifying the initial, later and complete healing stages in conjunction with the index derivative.

Conclusion: In this study, a two-sensor measurement strategy to quantify fixated femur healing is investigated. It is shown that the mass loading effect did not affect this vibrational analysis method ability to assess the state of healing, and both coherent bending and twisting modes associated with healing were easily identified. The proposed healing index, its derivative, and the cross-spectra are a viable tool for quantitative healing assessment.

Keywords

Bone healing assessment, structural health monitoring, vibration analysis, internal fixation, fracture healing assessment

Date received: 26 June 2017; accepted: 15 March 2019

Introduction

The advent of new imaging techniques for bone healing and union of fracture assessment, e.g. magnetic resonance imaging (MRI) and computed tomography (CT) scans, has not led to a definitive quantification of the state of healing and union of fractures.¹ Morshed¹ believes that the future direction of fracture healing assessment should focus on further validation of the currently available tools and development of better physician-assessed and patient-assessed instruments in the measurement of the union. In this respect, the work presented in this paper strives to provide evidence and validation in the use of vibration technique for the

¹Department of Mechanical & Aerospace Engineering, Monash University, Melbourne, Australia

²The Alfred Hospital, Melbourne, Australia

³The National Trauma Research Institute, The Alfred Hospital, Melbourne, Australia

⁴Faculty of Medicine, Nursing and Health Sciences, Monash University, The Alfred Hospital, Melbourne, Australia

⁵Trauma Service, The Alfred Hospital, Melbourne, Australia

Corresponding author:

WK Chiu, Monash University, Wellington Rd, Clayton, Victoria 3800, Australia.

Email: wing.kong.chiu@monash.edu

healing and state of union assessment of the bone fracture. The work presented is a systematic study to show how the state of healing of a fractured long bone (femur) treated with a rigid internal fixation affects the stiffness-related dynamic response. The science and knowledge derived are important for future development of the complementary application of a variety of techniques to critically assess the state of healing and union of fractures for the improved management of fractures.

The mechanical properties of long bones (e.g. femurs and tibiae) can be determined by its vibration characteristics.^{2,3} These techniques are based on the bending modes of the bone and are analogous to the beam bending in mechanical vibration. Whilst most studies reported on work performed on bones (e.g. femurs and tibiae) that are either excised or are artificial, Benirschke et al.⁴ included trials on patients which showed that the flexural rigidity of a tibia in bending could be related to its resonance frequency of first mode bending. The technique was highly reproducible in normal volunteers tested and there was no variability in resonant frequency measured on the right and left leg.

The work by Benirschke et al.⁴ led to an important observation that the change in resonant frequency is highly correlated with time post-injury in normally healing fractures. The ability to use this measurable quantity to quantify the state of healing is an important contribution to current strategies in the management of the treatment of a fracture. A form of non-invasive and non-radiative assessment will certainly be beneficial to patient care.

The physics behind the work by Benirschke et al.⁴ concurs with the findings of Richardson et al.,⁵ Miles et al.⁶ and Claes and Cunningham.⁷ These works related stiffness changes to the state of healing of long bones. Although Miles related the bending stiffness and the torsional stiffness of a femur to the state of healing, their femur was loaded statically. An understanding of this relationship from the dynamics response viewpoint is important for the development of a dynamics-based healing assessment methodology of an internally fixated femur. In order to facilitate the in-vivo measurement of a femur, some fundamental understandings on the relationship between the engineering quantities measured and the state of healing of a fixated femur are essential.

The works by Benirschke et al. and Richardson et al. led to some recent efforts to extend the concept of structural health monitoring of engineering structures to monitoring of the state of healing and union of a fixated fracture. When a femur is treated with an external fixation, Ong et al.^{8,9} showed that the dynamic response of the entire construct (i.e. femur + external fixation) is sensitive to the state of healing and union of the fractured region. Indeed, this work is aptly complemented by recent work by Mattei et al.¹⁰ who reported on the ability to assess the state of healing of an externally fixated

tibia. They provided some important insight into the choice of an excitation type and the appropriate excitation-response locations.

The two fixation techniques that are commonly used to treat a fractured bone are the intramedullary nail (IM nail) and the plate-screw system. The ability to monitor the state of healing and the union of the internally fixated fracture is indeed challenging. The challenges posed by the internal fixations are as follows:

- a. The internal fixation does not lend itself easily to instrumentation. This was demonstrated by Nemchand¹¹ who performed animal trials but suffered a series of hardware failures highlighting the difficulty with instrumenting an internal fixation. While future development of sensor or sensory systems may remove this impediment, a quantitative healing assessment of an internally fixated fractured femur using externally mounted sensors represents an immediate challenge that needs to be addressed.
- b. Benirschke et al.⁴ highlighted some issues with using resonant frequency techniques to assess healing on internally fixated tibiae. They found that while tibiae fixed with relatively flexible 2-bar external fixator produced frequencies comparable to an intact tibia, the effect of unreamed tibial nails (i.e. internal fixation) depended on the fit of the nail. For this reason, they excluded patients with internal fixators in their trials.
- c. Tower et al.¹² found that tibiae treated by interlocking nails were frequently falsely identified as being healed by resonant frequency studies. They asserted that this technique is not useful in predicting healing when this fixation technique is used. They attributed this to the fact that the fixation construct of locked IM nail is rigid enough to mask the change in stiffness related to the healing of a fracture. Many of these fractures are falsely identified as being healed because the resonant frequency analysis may measure the stiffness of the fixation rather than fracture healing.

It must be emphasised that the above studies were focused mainly on the bending response of the bone.

Garnier et al.¹³ reported a limited amount of work on the torsion properties of human cancellous bone. They reported some tests performed on different sites showing the correlation of the apparent density of the bone and the shear modulus. Bone mineral density is noted to be one of the parameters that can be used as an indicator of bone healing.¹⁴ The work by Miles et al.⁶ related the state of healing to the bending and torsional stiffness of an internally fixated femur using a series of static tests. Accordingly, Chiu et al.¹⁵ reported on a series of computational work to show that the bending and torsional response of an internally fixated femur may be used to assess its state of healing and union. A definitive

set of experiments is required to show that the torsional response is a useful quantity that can assist with the healing assessment methodology. Furthermore, the results must show that the frequency response must be directly related to the changing mechanical properties of the bone arising from healing.

In pursuing this mechanical-based assessment methodology that is based on the dynamic response of the fixated bone, the problems with soft tissue and interpretation of vibration-based results which have persisted to this day must be addressed (see also Nokes¹⁶). The soft tissue manifests itself as mass loading and damping on the mechanical structure (i.e. femur) (Ong et al.⁹). An inability to address this mass loading and damping issue will limit the applicability of the assessment technique for clinical use. Tsuchikane¹⁷ recognized that surrounding soft tissues and the joints absorbed the vibrations in the tibia. He reported that muscles were the most significant dampers significant in this experiment. According to Tsuchikane,¹⁷ the main contribution from soft tissue and joints that affected the vibration response of the tibia in a body is the increase in the 'apparent' weight of the tibia (i.e. mass loading). The resonant frequency was primarily dependent on the weight of the leg but it was also influenced by the individual ligaments at the knee joint. It was shown that soft tissue, the joints and fibula essentially increased the 'apparent' weight in the theoretical vibrational equation, and played a role in the dampening of the tibial vibrations. The damping effects caused by mass loading are illustrated by Zhang et al.¹⁸

Tsuchikane¹⁷ recognized that the tibia had a primary single bending mode and its mode shape was not influenced by the knee joint, ankle joint and the fibula if the leg was suspended. This suggests that a change in the resonant frequency of the tibia in vivo represents a change in the condition of the tibia itself. This effect was also reported by Ong et al.^{8,9} where they found that the mass loading can affect the dynamic response of an externally fixated fractured femur. However, the state of union and healing can be identified from its dynamic response.

The aim of this work is to provide evidence that the dynamic response that includes both bending and torsional vibration of an internal fixated femur which can be used to identify the state of healing and union. Two composite femurs, which exhibit similar properties of bones,¹⁹ fixated with an IM Nail and a plate-screw system will be used in this study. The osteotomised region of the fixated femur will be filled with a slow curing epoxy (30-min cure time) to simulate bone healing. It will be shown that the delayed union of the fixated femur can be identified and characterised. The robustness of the healing assessment methodology will be assessed with the mass loading of the fixated femur

with modelling clay. The modelling clay is introduced to simulate the effects of soft tissue (see also Ong et al.⁹).

Plate fixation

The experimental setup shown in Figure 1 was constructed to reveal as many vibrational modes as possible. A fixed boundary condition at the head of the femur was approximated by clamping in a vice which has been fastened to a rigid table. A secure grip with the vice is achieved by using 3D printed vice jaws matched to the femur head geometry. Two unidirectional accelerometers (B&K Type 4507) which have been orientated to measure acceleration in the Y-axis direction were attached to the test specimen. The excitation was provided by an instrumented impact hammer (B&K Type 8206) struck at the labelled location downward in the X-axis direction. Given the geometry of the femur, this form of excitation will induce both bending and torsional modes. Therefore, the 2-sensor measurement strategy will provide information on both the magnitude and the phase of the dynamic response. The voltage from the accelerometers and impact hammer was recorded and processed by a 6-channel B&K Pulse.

An AxSOS small fragment locking system (shown in Figure 2) from Striker Corporation was used to fixate the femur during healing. The fixation was installed with six stainless steel screws while the femur was intact. The femur was osteotomised using a saw blade and the tape was placed over the cut to form a mould which could be filled with epoxy adhesive. At this point,

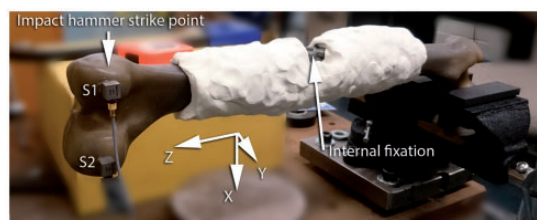


Figure 1. Experimental setup.

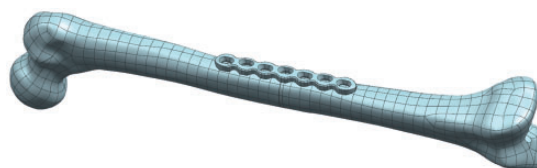


Figure 2. Illustration of the plate-screw system fixated the fractured femur.

modelling clay was added to the femur as shown in Figure 1 with a gap intentionally left at the cut. This gap allowed inclusion of the epoxy adhesive which is used to simulate the healing of the osteotomised region. The modelling clay used is a dense and soft plasticine to imitate the effects of mass-loading and damping due to soft tissues.⁸ The tightly moulded modelling clay around the femur can be removed after the experiment. Two-part epoxy with a curing time of 30 min was then prepared and then inserted into the cut. Once the cut is completely filled, the gap in the modelling clay is filled to make a uniform layer around the femur. It is expected that the time taken to prepare the specimen preparation will vary. The mass of clay used is approximately 1 kg. The final mass of the Sawbone femur, fixation and modelling clay is tabulated in Table 1.

The chemical reaction begins upon mixing of the two parts. The commencement of the experiment would be the time referred to as “0 minute”. The dynamic

response of the fixated femur was taken at regular intervals as the epoxy cures and “heals” in the osteotomised region in the femur. During these tests, the cross-spectrum (between accelerometers S1 and S2) and the coherence of the data from the two accelerometers were acquired at 5-min intervals. This was done up to 155 min after mixing the epoxy in order to span the entire curing process. The measurement settings were as follows: frequency bandwidth of 10 kHz, frequency resolution of 1.56 Hz and the spectra were averaged over 10 samples to obtain a good signal-to-noise ratio. It should be noted that the spectrum was observed to stabilise after an average of 7 samples. It should be noted that the measurement at each state of healing takes approximately 30 s. This is not significant compared with the curing time of the adhesive.

The cross-spectrum results “without mass loading” are first presented in Figure 3 for reference. Figure 3 shows the cross-spectrum power spectral density (PSD) and the coherence of the sensors obtained from a “fully” healed fixated femur without the addition of modelling clay (i.e. no mass loading). The y-axis phase of the cross-spectrum is ranged from $(-\pi, +\pi)$. The phase plot is used to indicate if the response measured at S1 and S2 are “in-phase” (which indicates a pure bending mode) or “out-of-phase” (indicating a pure torsional or twisting mode). The coherence

Table 1. Mass of test specimen with plate fixation.

Sawbone femur	512 g
Sawbone femur + fixation	600 g
Sawbone femur + fixation + clay	1600 g

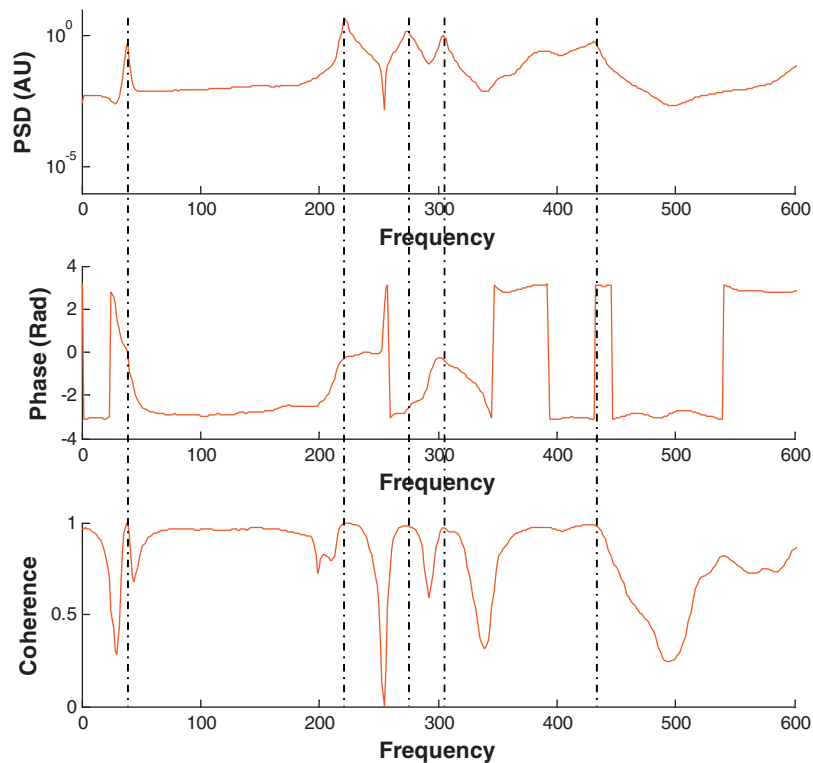


Figure 3. Cross-spectrum for femur bone with plate-screw fixation without modelling clay.

function was also added to the results which is calculated by

$$\text{coherence}(f) = \frac{|CS(f)^2|}{S1(f)S2(f)} \quad (1)$$

Coherece helps to determine the causality between readings from S1 and S2. A coherence value of > 0.95 between S1 and S2 will be achieved when these signals can be attributed to the response of the dynamic test specimen. This will help identify frequencies of the coherent modes.

The modes identified are as follows:

- The in-phase modes were identified at 37 Hz, 220 Hz and 305 Hz.
- The out-of-phase modes were identified at 275 Hz, 390 Hz and 431 Hz.
- The coherence at these frequencies is approximately 1.

These results will be used to assess the effects of mass loading on the dynamic response of the fixated femur. The cross-spectrum analysis obtained from this

experiment at the various stages of simulated healing is shown in Figure 4(a) and (b).

The main observations of the results are as follows:

- The first in-phase mode at 26 Hz is unaffected by the presence of the modelling clay and is unaffected by the state of simulated healing. Therefore, it does not lend itself to the monitoring of the state of healing or union of the fixated femur. The coherence associated with this mode did not change with time.
- When the fixated femur is fully healed (at 150 min in Figure 4(b)), the second in-phase mode is located at 155 Hz. The effects of mass loading are evident. Without the added modelling clay, this mode was observed at 220 Hz. It is also evident that this mode is sensitive to the state of healing of the fixated femur. It can be seen in Figure 4(a) and (b) that this mode shifted from 136 Hz to 155 Hz. The transition of the mode as a function of healing can be seen in Figure 4(a). The development of the coherence function of this mode can be seen to improve (approaches unity) with time. The shift in the frequency peak up to 60 min is due to the increase in stiffness and curing of the adhesive (e.g. 155 Hz). Beyond 60 min, the cross-spectra at this frequency

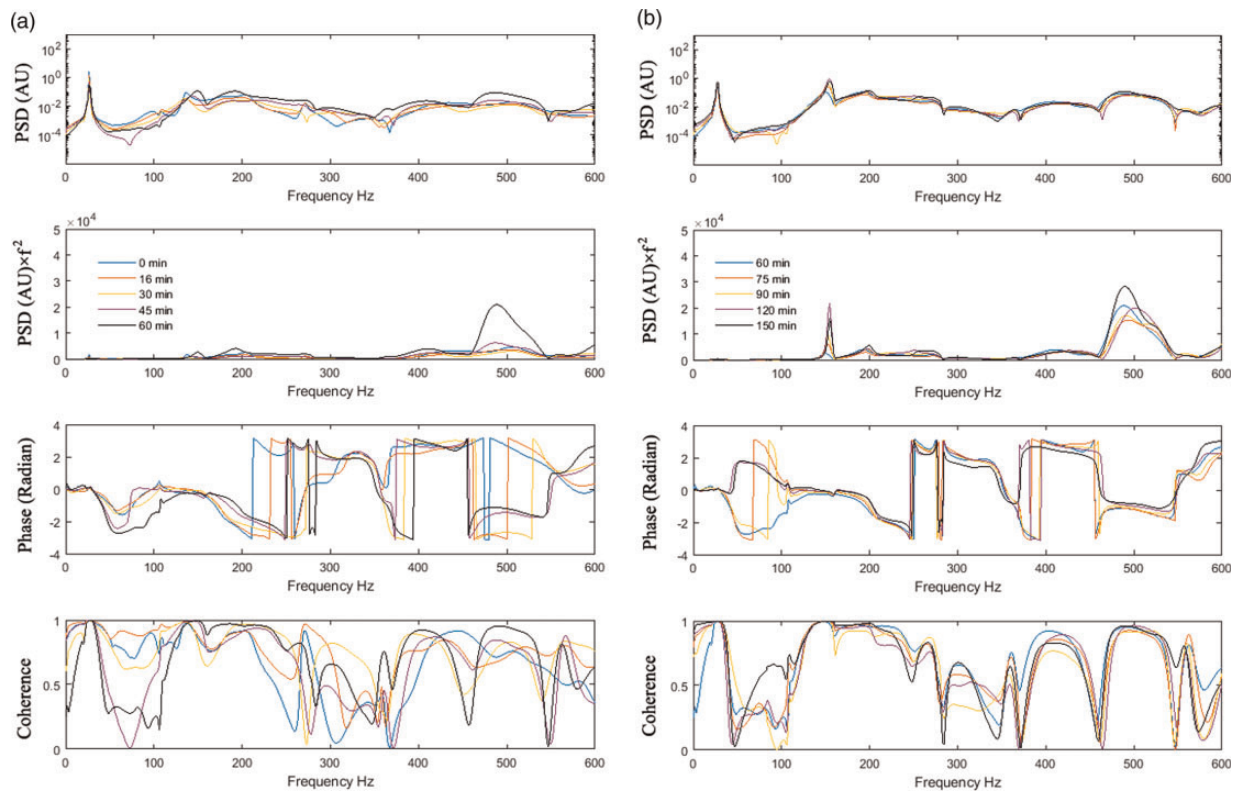


Figure 4. Cross-spectrum and coherence functions for femur with plate-screw fixation (with modelling clay). (a) 0–60 min; (b) up to 150 min.

simply increased in magnitude. This can be attributed to the reduction in damping as the adhesive achieves full cure. This is consistent with the properties of the epoxy used which is known to achieve full cure after 3 h.

- It is also evident that the higher frequency modes are affected by the added modelling clay. The cross-spectra shown in Figure 4(a) and (b) have revealed increasing contributions from the higher frequency modes as a function of healing. These modes are severely damped out by the modelling clay. Interestingly, the magnitude of the response at the higher frequency bandwidth (400–550 Hz) did not increase much after 60 min into the experiment. To enhance the visualisation, the magnitude of the spectra was weighted by frequency squared (f^2). The results in Figure 4(a) and (b) show that the development of the mode at approximately 480 Hz is sensitive to the state of healing of the fixated femur. The coherence is observed to asymptote to 1 with time. This shows that the response at this bandwidth is sensitive to the increased stiffness due to the adhesive cure. This effect is certainly not masked by the mass loading. It is also evident from these figures that the contribution of these modes to the overall spectra response is useful for the assessment of the state of healing of the fixated femur. The coherence at these higher frequency modes which is seen to approach unity with time attests to their presence and not merely as experimental artefacts. The phase plot indicated that the phase difference between the sensor S1 and S2 is approximately 1.3 rad (74°). This suggests that this mode is not pure bending and has some degree of twisting motion. This is expected given the geometry of the femur.

These observations were used to formulate the healing index (HI) given by equation (2) and the normalised form in equation (3). The form of HI is adapted from the damage index presented in Lichtenwalner et al.²⁰ The frequency-weighted cross-spectrum PSD is

integrated over the 0–600 Hz range. This frequency range is chosen to capture all modes observed in Figure 4. The HI is normalised to the cross-spectrum at time zero (equation (3)). Figure 5 shows the results obtained when equations (2) and (3) were applied to the spectra shown in Figure 4. This plot indicates that a healed femur will return a healing index nearly 200% higher than a fractured fixated femur. This is a promising result for quantification of healing as the healing index is proportionate to the state of healing

$$\text{Healing Index } (t) = \int_0^{600} CS(f,t) \times f^2 df \quad (2)$$

$$\begin{aligned} HI(t) &= \text{Normalised Healing Index } (t) \\ &= \text{Healing Index } (t) / \text{Healing Index } (t = 0) \end{aligned} \quad (3)$$

$$HI_t(t) = \frac{d}{dt}(HI(t)) \quad (4)$$

In addition to the HI at each point in time, a solid line has been curve-fitted to show the trend of the HI. The time-derivative of the healing index (HI_t) curve is also presented in Figure 5(a) as calculated by equation (4). From the plot of HI_t , the following can be observed:

- Initial stages of healing (State A) – The material properties at the osteotomised region of the fixated femur are regaining stiffness and strength during the initial stages of simulated healing. This is represented by the monotonically increasing HI and HI_t .
- Later stages of healing (State B) – It is observed that the HI_t attains a local maximum at approximately 50 min (shown in Figure 5(a)). Referring to Figure 4(a) and (b), this is the time where the shape (i.e. frequency shift) of the cross-spectra has stabilised. Beyond this time, the energy within the spectra asymptotically fills up and can be attributed to the reduction in damping as the epoxy attains full cure (i.e. complete healing).

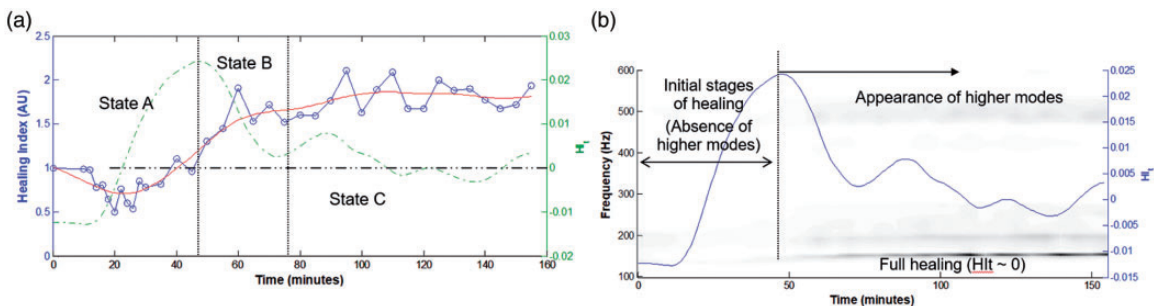


Figure 5. State of healing. (a) HI for femur with plate-screw fixation; (b) Cross-spectrum amplitude evolution and HI_t with time.

- Complete healing (State C) – the asymptotic value that the spectra (see Figure 4(b)) characterise the complete healing. The value of HI will asymptote and the value of the HI_t will be expected to be zero or near zero. This is confirmed by the results shown in Figure 5(a).

The results described above show that the viability of using the cross-spectrum of the two sensors arranged in Figure 1 to assess the state of healing of this internally fixated osteotomised femur. However, caution must be made when interpreting HI_t . This time derivative is susceptible to variation of the HI measured as a function of time. However, as the State A and State B are less susceptible to noise, it is recommended that the HI be assessed in conjunction with the development of the cross-spectra. This will greatly assist with the healing assessment of the fixated femur.

Figure 5(b) shows how the overlaying plots of the evolution of HI_t and cross-spectra are useful for assessing the state of healing of the femur. The axis on the right (HI_t) is associated with the solid line which depicts equation (3). Given that the cross-spectrum was acquired at 5-min intervals, the evolution of the cross-spectra which was in the form of an intensity plot was superimposed. The overlaid plots highlighted the

correlation between the point of inflexion of the HI curve and the formation of higher frequency modes.

The experiment was repeated to confirm the repeatability of these key observations. The resulting cross-spectrum data, HI and evolution of PSDs are shown in Figures 6(a) and (b) and 7(a) and (b). The features identified as key to the healing assessment are also observed here, namely:

- Similar dynamic responses were obtained at the frequency bandwidth in the vicinity of 150 Hz and 500 Hz as a function of simulated healing.
- The key features of the indices (HI and HI_t) with the overlaid spectra responses are also observed in the repeated test.

Intramedullary nail fixation

The IM nail fixation was a model T2 femoral nail obtained from the Stryker Corporation. The test procedure is identical to that previously used when studying the plate-screw fixated femur with modelling clay. However, this fixation is installed differently to the plate-screw fixation as shown in Figure 8. The IM nail is inserted into the cancellous core of the femur

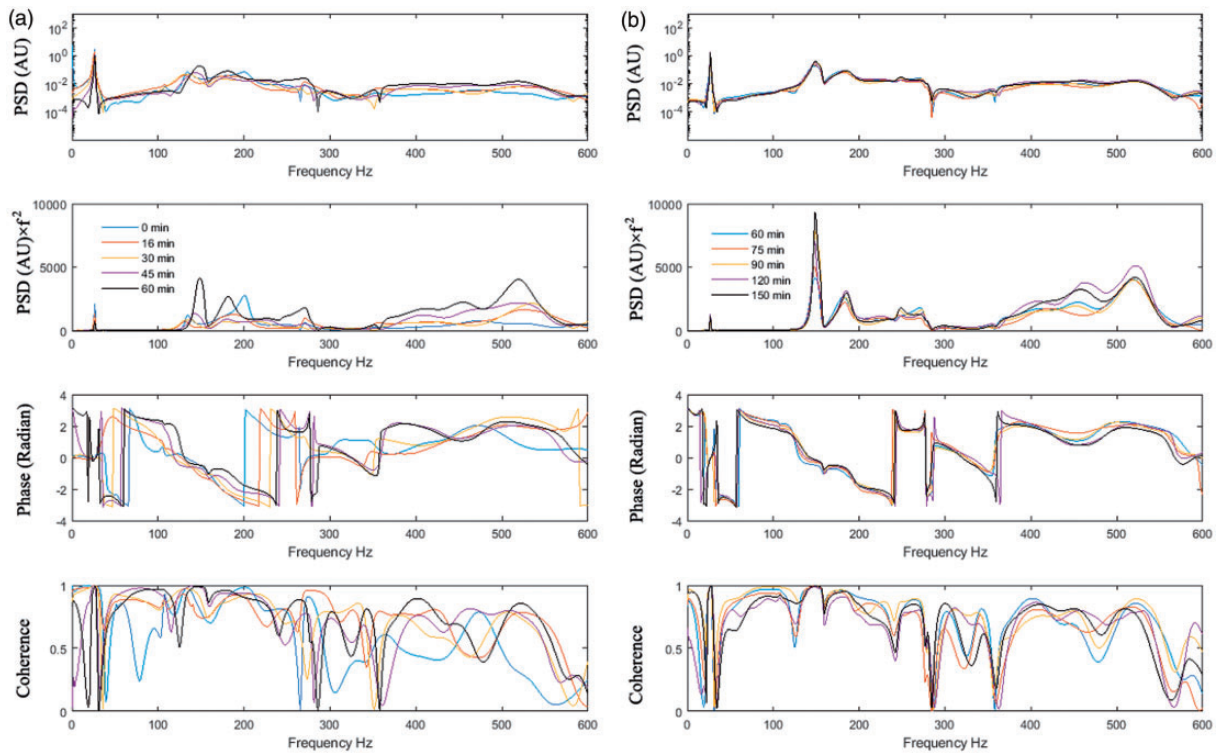


Figure 6. Cross-spectrum and coherence functions for femur with plate-screw fixation (repeated experiment). (a) 0–60 min; (b) up to 150 min.

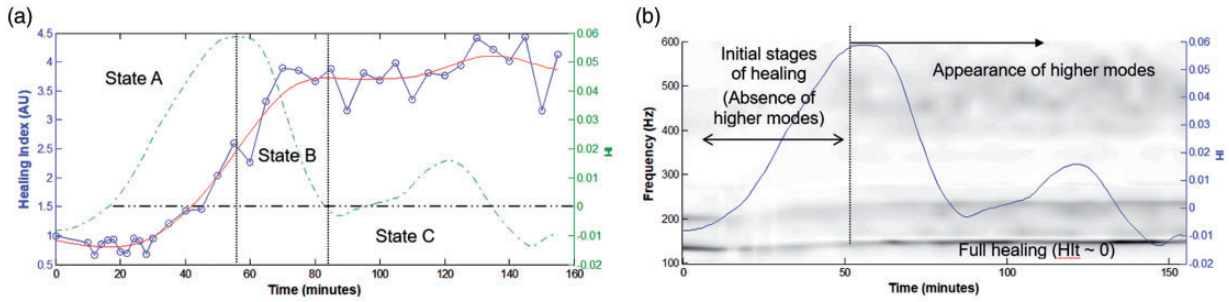


Figure 7. State of healing (repeated experiment). (a) Healing index for femur with plate-screw fixation; (b) Cross-spectrum amplitude evolution and HIt_t with time.

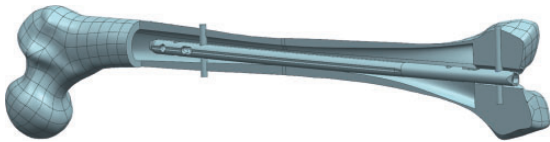


Figure 8. Illustration of femur with IM nail installed.

Table 2. Mass of test specimen with IM nail fixation.

Sawbone femur	512 g
Sawbone femur + fixation	638 g
Sawbone femur + fixation + clay	1638 g

and secured using two fasteners on each of the ends of the fractured femur. A new composite femur is used. The component weights are tabulated in Table 2.

As presented for the plate-screw fixation, the cross-spectrum PSD, phase and coherence were measured over a period of 155 min during the simulated healing experiment.

Figure 9 shows the cross-spectrum and the coherence of the sensors obtained from a “fully” healed femur without the addition of modelling clay (i.e. no mass loading) for reference. The modes identified are as follows:

- The in-phase modes were identified at 39 Hz and 230 Hz.
- The out-of-phase modes were identified at 260 Hz, 369 Hz and 416 Hz.
- The coherence at these frequencies is approximately 1.

The results obtained from the fixated femur with the addition of the modelling clay are shown in Figure 10(a) and (b) for regular time intervals. These results show the development of cross-spectrum and the coherence function obtained at various times during the simulated healing. As in the above section, the

cross-spectrum is weighted by f^2 to highlight the contribution from the higher frequency modes. The main observations of the results are as follows:

- As in the previous case, the first in-phase mode at 28 Hz is unaffected by both the presence of the modelling clay and the state of simulated healing. Therefore, it does not lend itself to the monitoring of the state of healing or union of the fixated femur.
- On complete healing, the second in-phase mode is located at 155 Hz. The effects of mass loading are evident. Without the added modelling clay, this mode was observed at 230 Hz. It is also evident that this mode is sensitive to the state of healing of the fixated femur. It can be seen in Figure 10(a) and (b) that this mode shifted from 136 Hz to 155 Hz when it is fully healed. The transition of the mode as a function of healing is shown in Figure 10(a). The coherence value at these frequencies is approximately unity at the later stages of the experiment.
- There is also the appearance of an out-of-phase mode occurring at 208 Hz shown in Figure 10(b). This has shifted from 260 Hz (see Figure 9) and can be attributed to the effects of mass loading. It should be noted that this mode only appears in the later stages of healing. Along with the mode at 155 Hz, they should be useful for healing assessment.
- It is also evident that the higher frequency modes are affected by the added modelling clay. The cross-spectra shown in Figure 10(a) and (b) displayed an increasing contribution from the higher frequency modes, between 400 and 550 Hz, as a function of simulated healing. The presence of the modelling clay severely affected the magnitude of the response. However, it is evident from these results that the contribution of these modes to the overall spectra response may still be useful in the assessment of the state of healing of the fixated femur. The coherence of close to unity at these higher frequency modes attests to their presence and not merely as experimental artefacts. The phase plot indicated

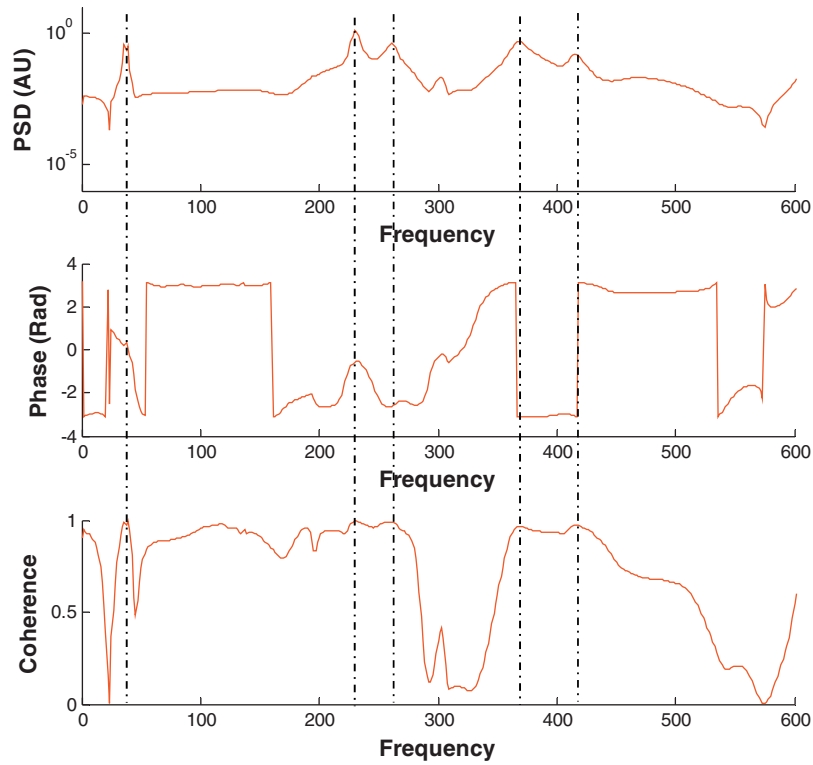


Figure 9. Cross-spectrum data for femur with IM nail without modelling clay (i.e. no mass loading).

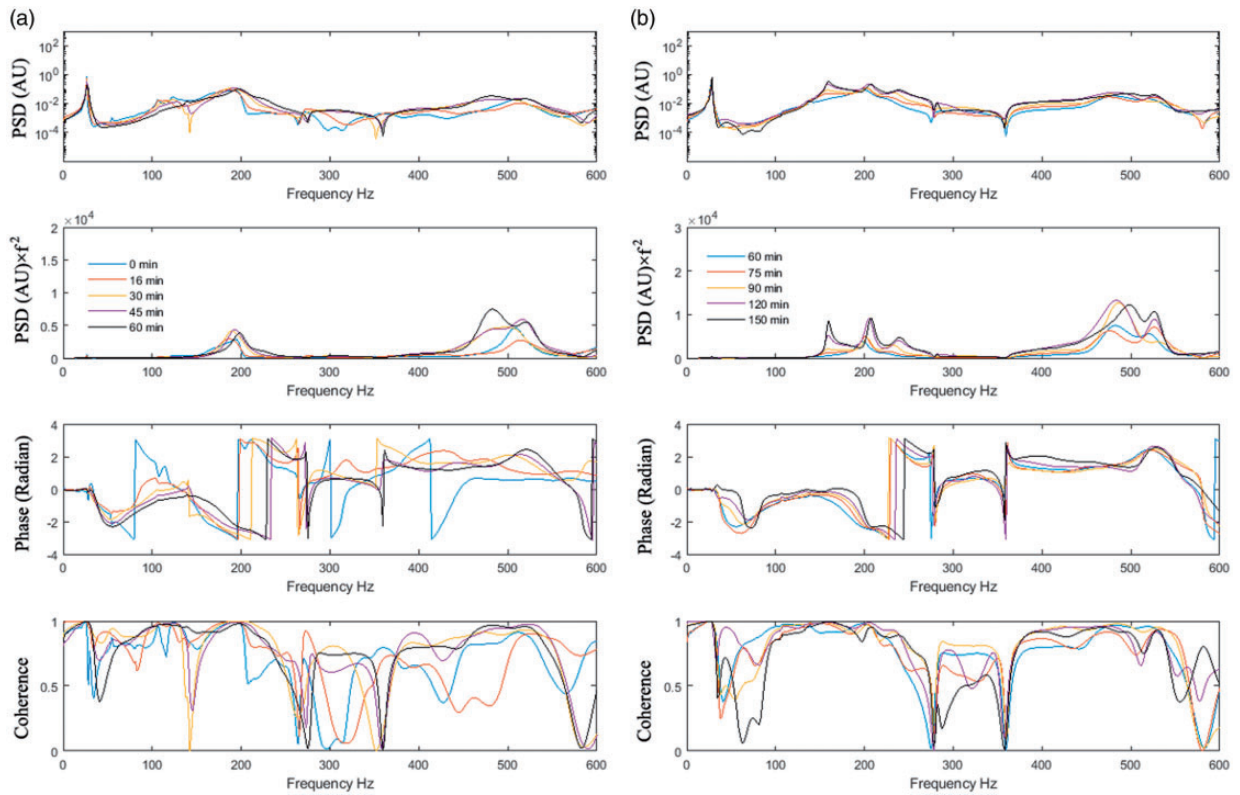


Figure 10. Cross-spectrum and coherence functions for femur with IM Nail. (a) 0–60 min; (b) up to 150 min.

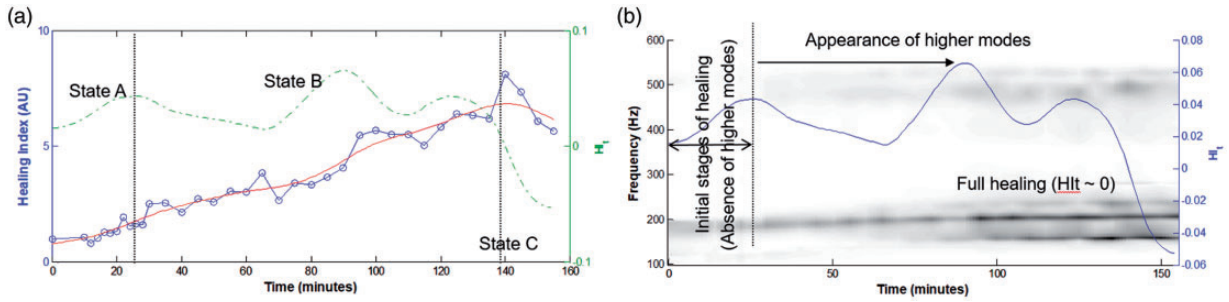


Figure 11. State of healing. (a) Healing index for femur with IM Nail; (b) Cross-spectrum amplitude evolution and HI_t with time.

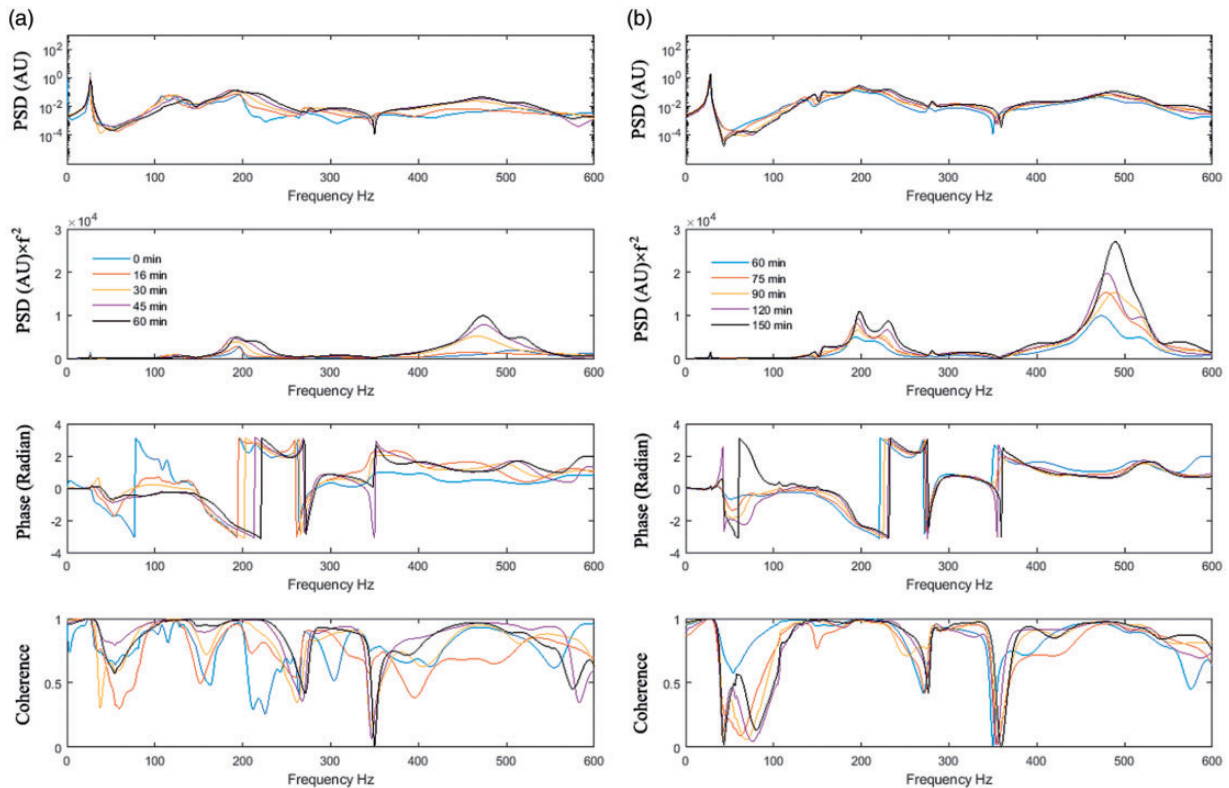


Figure 12. Cross-spectrum and coherence functions for femur with IM Nail (repeated experiment). (a) 0–60 min; (b) up to 150 min.

that the phase difference between the sensor S1 and S2 is approximately 2.6 rad (150°) suggesting that there is significant degree of twisting motion.

- The spectra when weighted by f^2 assisted with the visualisation of the development of the spectra in the range between 400 and 550 Hz. These results in Figure 10(a) and (b) show that the development of the mode at approximately 480 Hz is sensitive to the state of healing of the fixated femur. The coherence is observed to asymptote to 1 with time.
- As observed for the plate fixation, the development of the spectra appears to stabilise after 60 min into the experiment. After this time, the magnitude of the

modes increases and can be attributed to the reduction in damping as the epoxy achieves full cure.

The HI and its time-derivative, HI_t , are presented in Figure 11(a). The HI_t curve clearly shows the various states during healing as described earlier. Figure 11(a) shows the overlaid plot of HI_t and the evolution of the cross-spectra with respect to the healing of the femur. The entire series of cross-spectra PSDs measured during the experiment are presented in this intensity plot. The HI gradient has also been overlaid which highlights the correlation between the peak gradient,

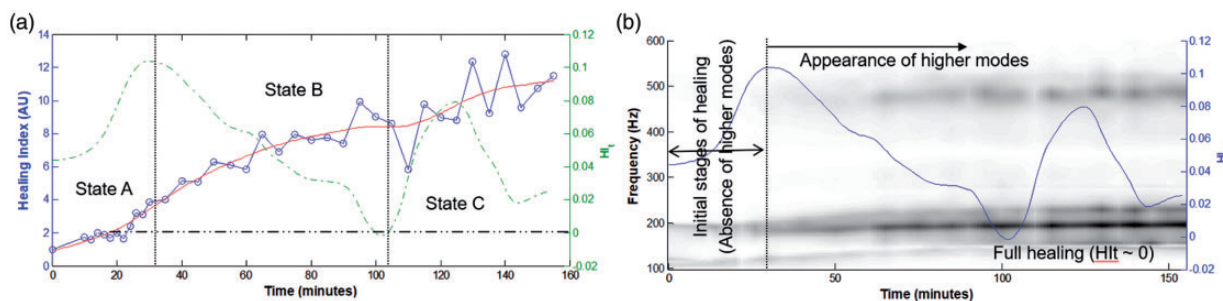


Figure 13. State of healing. (a) Healing index for femur with IM nail; (b) Cross-spectrum amplitude evolution and HI_t with time.

the formation of higher frequency modes, the increase in the frequency of pre-healing modes and an increase in PSD for all modes.

The significance of incorporating HI_t and the evolution of the cross-spectra for healing assessment is shown in Figure 11(b). Overlaying the value of the HI, HI_t and the evolution of the cross-spectra, the state of healing can clearly be identified. As shown in both Figure 11(a) and (b), State A of the healing process terminated at approximately 30 min into the experiment. This is consistent with the cross-spectra results shown in Figure 10(a) and (b). It was also observed that the shape of the cross-spectra stabilised about 30 min into the experiment.

The experiment was repeated to confirm the repeatability of these key observations. The resulting cross-spectrum data, HI and evolution of PSDs are shown in Figures 12(a) and (b) and 13(a) and (b). It is evident that the observations discussed above are repeatable.

Discussions

The use of dynamic responses of long bones to define its state of healing was reported by many researchers including Benirschke et al.⁴ and Miles et al.⁶ The results presented in this paper augur well with these earlier works especially with those of Miles et al. The sensor arrangement presented in this paper showed how the dynamic modes (both bending and torsional) can be determined and utilised to assess the state of healing of an internally fixated long bone. The results provided some insight into the use of these dynamic responses to determine its state of healing. The state of healing of the mass-loaded fixated fractured femur is found to have an effect on its dynamic response. To assist with the interpretation of these results for healing assessment purposes, an HI was proposed. It is evident from the investigations described above that the presentation of the HI, its time-derivative along with the time evolution of the cross-spectrum (see Figures 5(a) and (b), 7(a) and (b); 11(a) and (b) and 13(a) and (b)) can yield a potential non-radiative assessment tool to complement

existing techniques of healing assessment. These results will provide a useful guide for the development of an extra-corporeal measurement strategy for the healing assessment of internally fixated long bones. Animals and clinical trials will be required to further tests and develop this healing assessment procedure.

Conclusion

The results presented provide evidence that the dynamic response that includes both bending and torsional vibration of an internal fixated femur can be used to identify the state of healing and union of an internally fixated femur. The works presented show the potential in determining the state of healing of two types of internally fixated femurs where modelling clay was added to simulate the mass and damping of soft tissue. The effects of mass loading are shown to compress the modes along the frequency axis. However, this mass loading effect did not affect the ability to assess the state of healing of the fixated femur using the dynamic response of the fixated femur as a driving principle. The dynamic responses used included both the bending and twisting motion of the fixated femur. A healing index is proposed to assess the state of healing. It was found that the simultaneous consideration of the time-derivative of the healing index and the time evolution of the cross-spectra are a viable tool for healing assessment.

Declaration of conflicting interests

The author(s) declared no potential conflicts of interest with respect to the research, authorship, and/or publication of this article.

Funding

The author(s) disclosed receipt of the following financial support for the research, authorship, and/or publication of this article: This project is funded by the US Navy Office of Naval Research (N00014-16-1-2882). The financial support provided is gratefully acknowledged.

Guarantor

WKC.

Contributorship

WKC, MR and MF conceived the idea for the research. WKC was responsible for the mechanical engineering aspects of the work. MR & MF ensured the clinical relevance of the work and the presentation of the results. WHO was responsible for the computational modelling, development of the software and in setting up the experiments. He directed TT in executing of the test plans. WKC and WHO wrote the first draft of the manuscript. All authors reviewed and edited the manuscript and approved the final version of the manuscript.


Acknowledgements

We would like to thank Dr B. S. Vien and Dr Z. K. Chiu for their assistance in this research and for proof reading of the manuscript.

ORCID iD

WK Chiu  <http://orcid.org/0000-0002-4359-2814>

WH Ong  <http://orcid.org/0000-0003-3625-5403>

M Fitzgerald  <http://orcid.org/0000-0003-0183-7761>

References

- Morshed S. Current options for determining fracture union. *Adv Med* 2014; 2014: 12.
- Vanderperre G and Cornelissen P. On the mechanical resonances of a human tibia invitro. *J Biomech* 1983; 16: 549–552.
- Vanderperre G, Vanaudekercke R, Martens M, et al. Identification of invivo vibration modes of human tibiae by modal-analysis. *J Biomech Eng* 1983; 105: 244–248.
- Benirschke SK, Mirels H, Jones D, et al. The use of resonant frequency measurements for the noninvasive assessment of mechanical stiffness of the healing tibia. *J Orthopaed Trauma* 1993; 7: 64–71.
- Richardson JB, Cunningham JL, Goodship AE, et al. Measuring stiffness can define healing of tibial fractures. *J Bone Joint Surg* 1994; 76B: 389–395.
- Miles AW, Eveleigh RJ, Wight BJ, et al. An investigation into the load transfer in interlocking intramedullary nails during simulated healing of a femoral fracture. *Proc Inst Mech Eng Part H* 1994; 208: 19–26.
- Claes LE and Cunningham JL. Monitoring the mechanical properties of healing bone. *Clin Orthopaed Relat Res* 2009; 467: 1964–1971.
- Ong WH, Chiu WK, Russ M, et al. Extending structural health monitoring concepts for bone healing assessment. *Fatigue Fract Eng Mater Struct* 2016; 39: 491–501.
- Ong WH, Chiu WK, Russ M, et al. Chiu, Integrating sensing elements on external fixators for healing assessment of fractured femur. *Struct Control Health Monitor* 2016; 23(12): 1388–1404.
- Mattei L, Longo A, Di Puccio F, et al. Vibration testing procedures for bone stiffness assessment in fractures treated with external fixation. *Ann Biomed Eng* 2017; 45: 1111–1121.
- Nemchand JL. Smart implant: the biomechanical testing of instrumented intramedullary nails during simulated callus healing using telemetry for fracture healing monitoring. Doctorate Thesis, Brunel University London, UK, 2015.
- Tower SS, Beals RK and Duwelius PJ. Resonant-frequency analysis of the tibia as a measure of fracture-healing. *J Orthopaed Trauma* 1993; 7: 552–557.
- Garnier KB, Dumas R, Rumelhart C, et al. Mechanical characterization in shear of human femoral cancellous bone: torsion and shear tests. *Med Eng Phys* 1999; 21: 641–649.
- Babatunde OM, Fragomen AT and Rozbruch SR. Noninvasive quantitative assessment of bone healing after distraction osteogenesis. *HSS J* 2010; 6: 71–78.
- Chiu WK, Ong WH and Russ M. Vibrational analysis of internally fixated femur to monitor healing at various fracture angles. *Proc Eng* 2017; 188: 408–414.
- Nokes LDM. The use of low-frequency vibration measurement in orthopaedics. *Proc Inst Mech Eng H* 1999; 213: 271–290.
- Tsuchikane A, Nakatsuchi Y and Nomura A. The influence of joints and soft tissue on the natural frequency of the human tibia using the impulse response method. *Proc Inst Mech Eng H* 1995; 209: 149–155.
- Zhang ZY, Zhu PY and Bao XY. The mass loading effect on lightweight cantilever mode frequency measurement by optical fiber sensor. *Photonics North* 2008; 2008: 7099.
- www.sawbones.com/products/biomechanical.html (accessed 25 March 2019).
- Lichtenwalner PF, Dunne J, Becker R, et al. Active damage interrogation for structural health monitoring. In: *Proc SPIE* 1997; 3044: 186–194.